International Journal of Earth, Energy and Environmental Sciences
ISSN: 2517-942X
Vol:11, No:9, 2017

# Discrete Element Modeling of the Effect of Particle Shape on Creep Behavior of Rockfills

Yunjia Wang, Zhihong Zhao, Erxiang Song

***Abstract*—**Rockfills are widely used in civil engineering, such as dams, railways, and airport foundations in mountain areas. A significant long-term post-construction settlement may affect the serviceability or even the safety of rockfill infrastructures. The creep behavior of rockfills is influenced by a number of factors, such as particle size, strength and shape, water condition and stress level. However, the effect of particle shape on rockfill creep still remains poorly understood, which deserves a careful investigation. Particle-based discrete element method (DEM) was used to simulate the creep behavior of rockfills under different boundary conditions. Both angular and rounded particles were considered in this numerical study, in order to investigate the influence of particle shape. The preliminary results showed that angular particles experience more breakages and larger creep strains under one-dimensional compression than rounded particles. On the contrary, larger creep strains were observed in he rounded specimens in the direct shear test. The mechanism responsible for this difference is that the possibility of the existence of key particle in rounded particles is higher than that in angular particles. The above simulations demonstrate that the influence of particle shape on the creep behavior of rockfills can be simulated by DEM properly. The method of DEM simulation may facilitate our understanding of deformation properties of rockfill materials.

***Keywords*—**Rockfills, creep behavior, particle crushing, discrete element method, boundary conditions.

## I. Introduction

Rockfills have been widely used in civil engineering, such as dams, railways and airport foundations in mountain areas since last century. A large number of field observations concerning rockfill behavior showed that the mechanical behavior of rockfill is time-dependent, and the post-construction settlement continues for many decades [1], [2]. It is widely accepted that particle breakage is the main cause of rockfill creep behavior, and much effort was put into testing rockfill samples in the laboratory to investigate the effects of particle size, strength and shape, water condition and stress level [3]. However, the microscopic mechanism of rockfill creep behavior still remains poorly understood.

Compared to physical experiments, the particle-based DEM provides the possibility to observe and monitor the microscopic rockfill response at an individual particle level. Considering that the particle breakage is the main cause of rockfill creep, there are mainly two ways to simulate rock aggregates: (1) using a breakable bonded cluster to model the particle [4], (2) replacing the original unbreakable disk or clump with a set of smaller disks [5], [6]. To simulate the time-dependent behavior of rockfill, Alonso et al. [7] developed a DEM model in which grains are characterized by clumps and the breakage criterion involves the subcritical propagation of fissures in the grain. Tran et al. [8] and Potyondy [9] modeled rockfill creep by incorporating bond-ageing models into particle mechanics method, reducing either parallel bond strength or bond diameter.

The above achievements demonstrated that the particle-based DEM is able to model the rockfill creep behavior. In recent studies, Zhao and Song and Zhou and Song investigated the effect of water condition and stress levels on rockfill creep behavior [10], [11]. As one of the important properties of rockfill, the influence of particle shape on rockfill behavior has been rarely studied. Zhou et al. [12] studied the effect of particle shape on peak strength of rockfill using a 3D DEM. However, the influence of particle shape on creep behavior has not been reported in the previous studies. The main objective of this paper is to investigate the influence of particle shape on rockfill creep behavior under different boundary conditions.

## II. Methodology

In this study, the commercial software Particle Flow Code in two dimensions (PFC2D, Itasca, 2008) was used to simulate rockfill aggregates. In order to simulate particle breakage, rock can be represented by clusters, which consist of a number of disks that bonded together. Considering the contact force and moment in a cluster, parallel bond was used. Each parallel bond has five parameters: normal and shear stiffness, normal and shear strength and radius. Once the normal or shear stress exceeds bond strength, the bond breaks, and a micro-crack appears. More details about the bond model can be found in Potyondy and Cundall [13].

To simulate the rockfill creep due to particle crushing, a few bond-ageing models have been proposed in [8], [9], [14], [15]. According to Zhao and Song [10], all those bond-ageing models can be used to simulate rockfill creep with appropriate empirical parameters. In this study, the bond-ageing model proposed by Tran et al. [8] was used, i.e. reducing parallel bond strength with time.

$$\sigma_b^t = \begin{cases} \sigma_b^0 & \sigma_n < \beta_1 \sigma_b^0 \\ \sigma_b^0 \left[ 1 - \beta_3 \int_{t_0}^{t} \exp\left( \beta_2 \dfrac{\sigma_n}{\sigma_b^0} - \beta_1 \right) dt \right] & \beta_1 \sigma_b^0 \le \sigma_n \le \sigma_b^0 \\ 0 & \sigma_b^0 < \sigma_n \end{cases} \quad (1a)$$

Yunjia Wang, Zhihong Zhao, and Erxiang Song are with the Civil Engineering Department, Tsinghua University, Beijing 100084, China (e-mail: wangyj14@mails.tsinghua.edu.cn, zhzhao@mail.tsinghua.edu.cn, songex@mail.tsinghua.edu.cn).

$$\tau_b^t = \begin{cases} \tau_b^0 & \sigma_n < \beta_1\sigma_b^0 \\ \tau_b^0\left[1-\beta_3\int_{t_0}^{t}\exp\left(\beta_2\frac{\sigma_n}{\sigma_b^0}-\beta_1\right)dt\right] & \beta_1\sigma_b^0 \le \sigma_n \le \sigma_b^0 \\ 0 & \sigma_b^0 < \sigma_n \end{cases} \qquad (1b)$$

Equation (1) is the mathematical expressions.$\sigma_b^0$ and $\sigma_b^t$ are the short- and long-term normal strength, respectively; $\tau_b^0$ and $\tau_b^t$ are the short- and long-term shear strength, respectively; $\beta_1$, $\beta_2$ and $\beta_3$ are three empirical parameters, which depend on particle size, shape and material properties. $\beta_1$ controls the magnitude of activation stress. If the applied normal stress $\sigma_n$ is below the activation stress $\beta_1\sigma_b^0$, the strength reduction is not activated. If $\sigma_n$ is larger than the activation stress but smaller than the short strength, the strength reduction is activated, then the parallel bond strength decreases with time according to (1). When $\sigma_n$ exceeds short strength, the parallel bond breaks and a micro-crack appears. In this study, the time step in bond degradation calculation was fixed at a constant value of 100 seconds.

## III. Modelling

The numerical square specimens had an initial side length of 200 mm. Two different particle shapes were used: rounded particles proposed by Zhao and Song [10] and angular particles proposed by Zhou and Song [11]. Defining the longest distance between two points in particle as diameter, the diameter range of rockfill aggregates in both rounded and angular specimens was 6.82 mm to 11.18 mm, with the average of 9.18 mm. With an initial porosity of 0.3, 120 rounded particles and 213 angular particles were generated respectively. The main micro-parameters are listed in Table I. More details about the preparation of specimens can be found in [10], [11].

TABLE I
Micro-Parameters for Rockfill Aggregates

| Micro-parameter | Unit | Value |
|---|---|---|
| Number of aggregates | - | 120(rounded) 213(angular) |
| Density | kg/m$^3$ | 2230 |
| Contact modulus | GPa | 4.0 |
| Ratio of ball shear to normal stiffness | - | 0.4 |
| Contact friction coefficient | - | 0.3 |
| Parallel bond radius multiplier | - | 1.0 |
| Parallel bond modulus | GPa | 4.0 |
| Ratio of parallel bond shear to normal stiffness | - | 0.4 |
| Parallel bond normal strength, mean | MPa | 10.0 |
| Parallel bond normal strength, standard deviation | MPa | 3.0 |
| Parallel bond shear strength, mean | MPa | 10.0 |
| Parallel bond shear strength, standard deviation | MPa | 3.0 |
| Empirical parameters $\beta_1$, $\beta_2$ and $\beta_3$ | - | 0.4, 40 and $5\times10^{-11}$ |

After the specimens were created, one dimensional compression and direct shear test were simulated. During one dimensional compression, the lateral and bottom walls were fixed while the top wall moved down at a certain velocity to attain a desired stress level. A servo algorithm was employed to maintain a constant normal stress during creep. For the direct shear test, the desired normal and shear stresses were attained through moving the upper box. Then, the stresses kept constant using the servo algorithm. The lower box was fixed during the whole process. Once the creep simulation began, the force chains, the breakage of rockfill aggregates and the specimen deformations were monitored during the whole test.

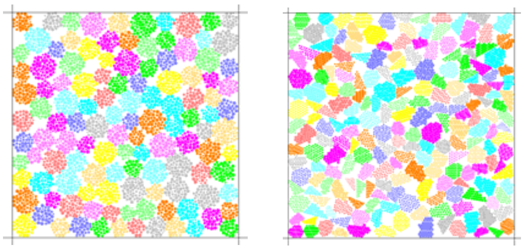

(a) Rounded specimen (b) Angular specimen

Fig. 1 Numerical rockfill specimens

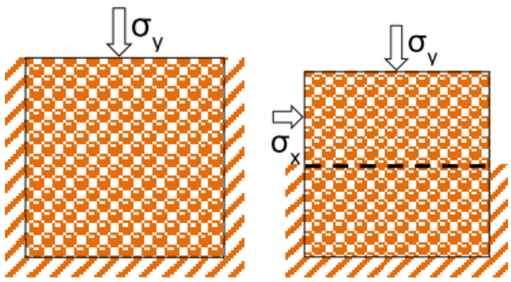


(a) One-dimensional compression (b) Direct shear

Fig. 2 Different boundary conditions

## IV. Results

### A. One Dimensional Compression

The normal stresses used in 1D compression were 400 kPa, 600 kPa, 800 kPa, 1000 kPa, and 1140 kPa, respectively. Eight angular specimens and six rounded specimens with different packing arrangements and bond strength were created by varying the seed of the random-number generator during material genesis.

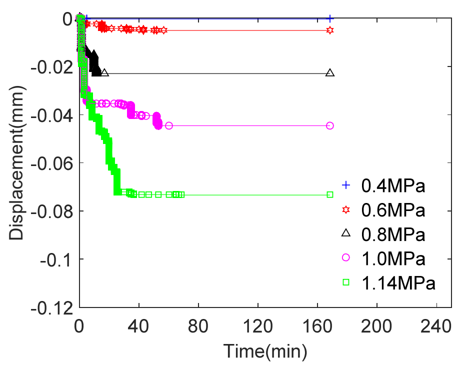


(a) Rounded specimens

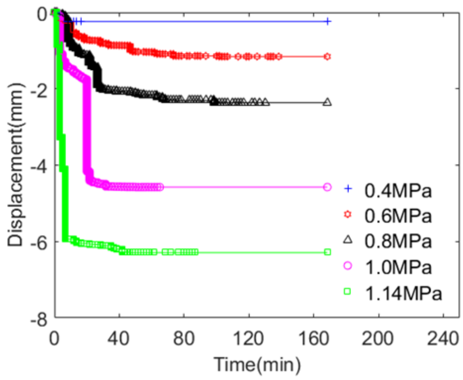


(b) Angular specimens

Fig. 3 Rockfill deformation under one-dimensional compression

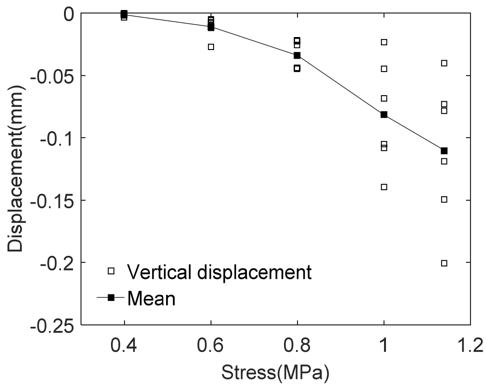


(a) Rounded specimens

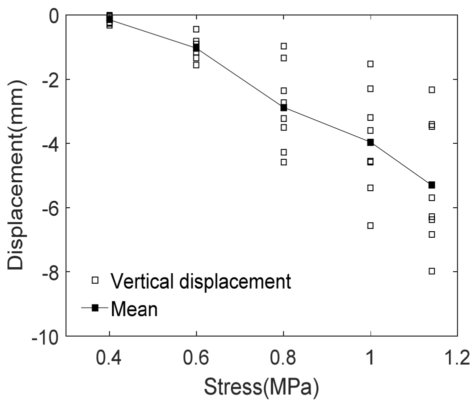


(b) Angular specimens

Fig. 4 Creep deformation under one dimensional compression at t=10000s

Fig. 3 shows the typical creep displacement-time curve under each constant normal stress. Both specimens showed an increasing normal displacement with the applied normal stress. Compared with rounded specimens, the angular ones experienced larger creep strains under the same normal stress. The normal displacements at 10000 seconds are compared in Fig. 4. Both angular and rounded particles showed an increasing average normal displacement with the applied stress; however, the increments of angular specimens were more significant. Fig. 5 shows the bond force distribution and micro-crack distribution under the normal stress of 0.8 MPa. Angular specimen had a more uneven distribution of force and experiences more breakages than rounded one, which could be responsible for the larger normal displacements of angular specimens.

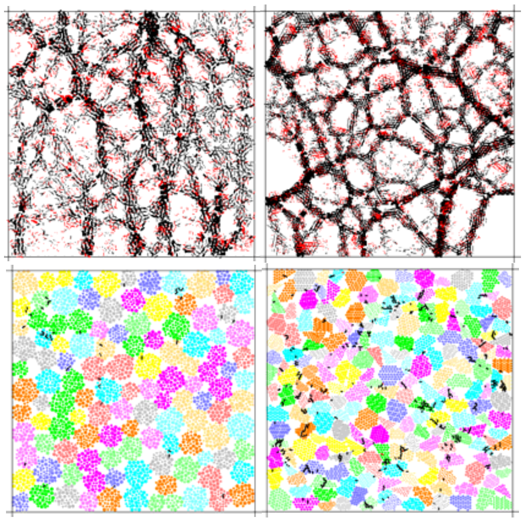

(a) Rounded specimen (b) Angular specimen

Fig. 5 Bond force and micro-crack distribution under one-dimensional compression

### *B. Direct Shear Test*

In the case of direct shear test, a constant normal stress of 1.14 MPa was applied on the upper box. The shear stress varies from 0.2 MPa to 0.6 MPa, and the interval is 0.1MPa. As in the previous case, eight angular specimens and six rounded specimens with different packing arrangements and bond strength were created.

Fig. 6 shows the typical displacement-time curves under different shear stresses. The deformation characteristics strongly depended on shear stress and particle shape. When the shear stress was low, both normal and shear displacements increased rapidly and then nearly remained constant, which could be considered the primary creep and secondary creep phases. At high shear stress, normal displacement was more significant than shear displacement. Both normal and shear displacements increased with the increasing shear stress; however, the increments of shear displacement of rounded specimens were more significant.

Fig. 7 shows the bond force and micro-crack distributions at t=10000 s under the shear stress of 0.5 MPa. In the rounded specimen, bond force was statistically more uniformly and micro-cracks formed mainly in the corner of particles. However, more micro-cracks appeared in the angular specimen, and more total fragmentation (particle splitting) was found on the force chains.

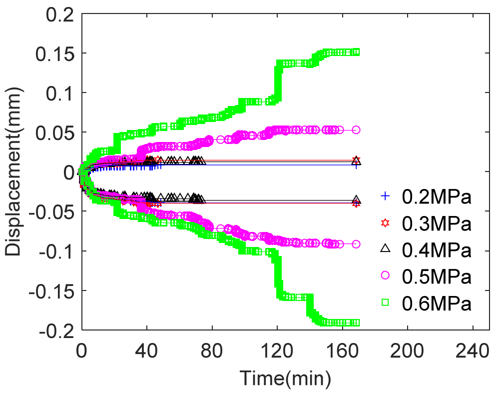


(a) Rounded specimens

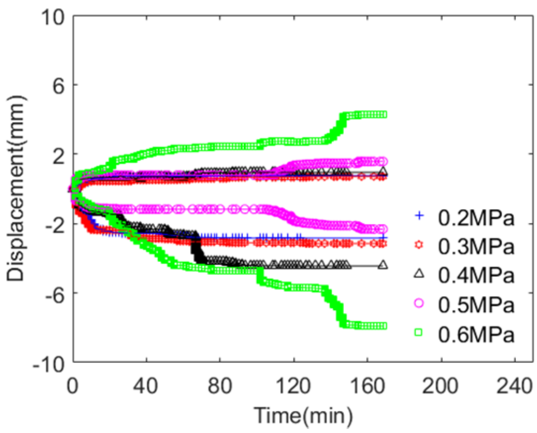


(b) Angular specimens

Fig. 6 Rockfill deformation under direct shear test

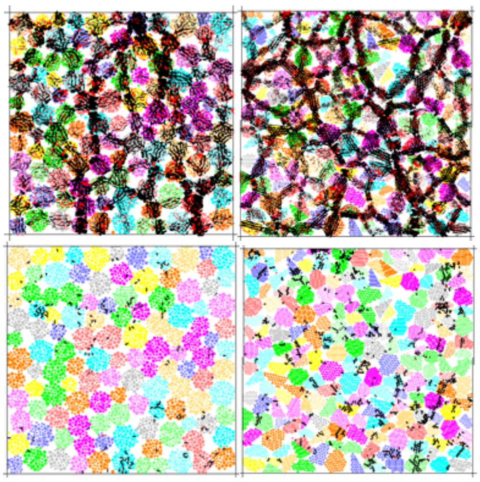

(a) Rounded specimen (b) Angular specimen

Fig. 7 Bond force and micro-crack distribution under direct shear test (shear stress=0.5 MPa)

All results at 10000 seconds are shown in Fig. 8, which includes the normal displacements from each test with lines joining the average values at each normal stress. Both angular and rounded particles showed an increasing average shear displacement with the applied shear stress. The average normal displacement that indicates the shear-induced contraction or dilatancy, however, did not exhibited a similar trend for angular and rounded particles. The average normal displacement of angular particle was nearly constant with increasing shear stress, while the normal displacement of rounded particles significantly increased with increasing shear stress. It is believed that the key particle plays an important role in the creep process in rounded particles.

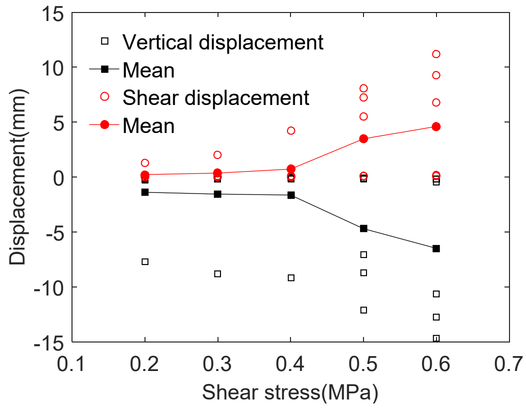


(a) Rounded specimens

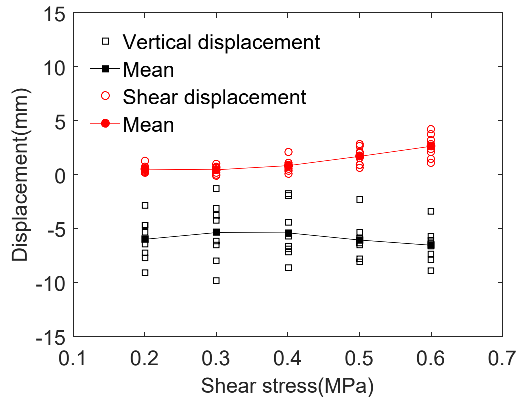


(b) Angular specimens

Fig. 8 Creep deformation under direct shear test at t=10000s

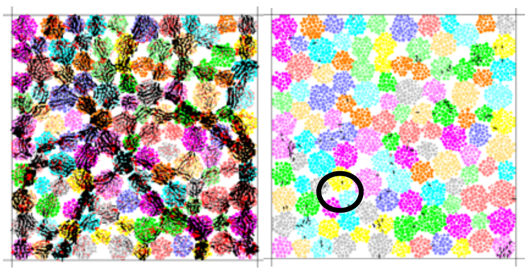

(a) At t= 10 mins

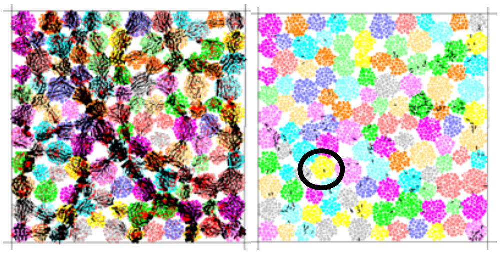

(b) At t= 30 mins

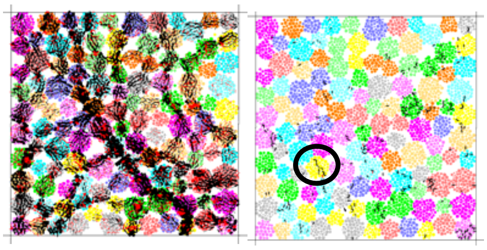

(c) At t= 40mins

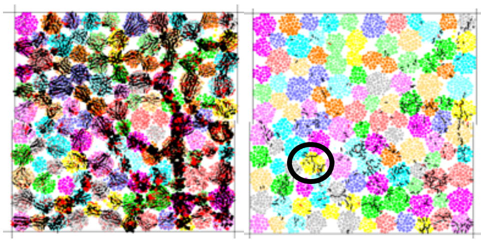

(d) At t= 50 mins

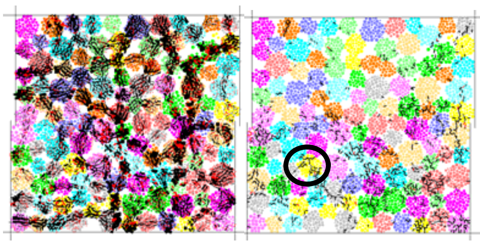

(e) At t= 60 mins

Fig. 9 Changes of bond force and micro-crack distribution (shear stress= 0.5 MPa)

In the force chain, a particle whose breakage could cause a chain reaction eventually leading to the failure of the sample can be defined as a key particle. Fig. 9 shows how the key particle works in rounded specimen during creep process. At t=10 mins, the force chain was stable and few micro-crack appeared. At t=30 mins, total fragmentation was found; however, the displacements were still small which meant that the specimen was still stable. At t=40 mins, the key particle was broken, leading to the change of force chains and resulting in lots of breakage in the next 10 minutes.

## V. Conclusions

In this study, the influence of particle shape on the creep behavior of rockfills with different boundary conditions was investigated using particle-based DEM. To simulate the creep behavior, the bond-ageing model proposed by Tran et al. [8] was used. Some detailed conclusions are drawn as below:

(1) Under one-dimensional compression, the normal displacement increased with normal stress. The displacements of angular specimens were more significant.
(2) Under direct shear test, both the normal and shear creep displacements of rounded particles were larger than that of angular ones.
(3) Key particle exists in both rounded and angular specimens; however, it plays a more important role in rounded specimens.

## Acknowledgment

This research is finically supported by the National Basic Research Program of China (973 Program, contract number2014CB047003).

## References

[1] Sowers, G. F., Williams, R. C., & Wallace, T. S. (1965, September). Compressibility of broken rock and the settlement of rockfills. In Proc. 6th ICSMFE (Vol. 2, pp. 561-565).
[2] Marsal, R. J., Arellano, L. R., Guzmán, M. A., & Adame, H. (1976). Infernillo: Behavior of dams built in Mexico. Instituto de Ingeniería, UNAM, Mexico.
[3] Oldecop, L. & Alonso, E. (2007). Theoretical investigation of the time-dependent behaviour of rockfill. Géotechnique 57, No. 3, 289–301.
[4] Cheng, Y. P., Nakata, Y., & Bolton, M. D. (2003). Discrete element simulation of crushable soil. Geotechnique, 53(7), 633-642.
[5] McDowell, G. R., & de Bono, J. P. (2013). On the micro mechanics of one-dimensional normal compression. Géotechnique, 63(11), 895.
[6] Tapias, M., Alonso, E. E., & Gili, J. (2015). A particle model for rockfill behaviour. Géotechnique, 65(12), 975-994.
[7] Alonso, E. E., Tapias, M., & Gili, J. (2012). Scale effects in rockfill behaviour. Géotechnique Letters, 2(3), 155-160.
[8] Tran, T. H., Vénier, R., & Cambou, B. (2009). Discrete modelling of rock-ageing in rockfill dams. Computers and Geotechnics, 36(1), 264-275.
[9] Potyondy, D. O. (2007). Simulating stress corrosion with a bonded-particle model for rock. International Journal of Rock Mechanics and Mining Sciences, 44(5), 677-691.
[10] Zhao, Z., & Song, E. X. (2015). Particle mechanics modeling of creep behavior of rockfill materials under dry and wet conditions. Computers and Geotechnics, 68, 137-146.
[11] Zhou, M., & Song, E. (2016). A random virtual crack DEM model for creep behavior of rockfill based on the subcritical crack propagation theory. Acta Geotechnica, 11(4), 827-847.
[12] Zhou, W., Ma, G., Chang, X., & Zhou, C. (2013). Influence of particle shape on behavior of rockfill using a three-dimensional deformable DEM. Journal of Engineering Mechanics, 139(12), 1868-1873.
[13] Potyondy, D. O., & Cundall, P. A. (2004). A bonded-particle model for rock. International journal of rock mechanics and mining sciences, 41(8), 1329-1364.
[14] Silvani, C., Désoyer, T., & Bonelli, S. (2009). Discrete modelling of time-dependent rockfill behaviour. International journal for numerical and analytical methods in geomechanics, 33(5), 665-685.
[15] Kwok, C. Y., & Bolton, M. D. (2013). DEM simulations of soil creep due to particle crushing. Géotechnique, 63(16), 1365-1376.